

Magnetic properties of interacting nanoparticles in a triangular lattice: Monte Carlo simulationsW. Figueiredo^{1,2} and W. Schwarzacher²¹*Departamento de Física, Universidade Federal de Santa Catarina, 88040-900 Florianópolis, Santa Catarina, Brazil*²*H. H. Wills Physics Laboratory, University of Bristol, Tyndall Avenue, Bristol BS8 1TL, United Kingdom*

(Received 4 July 2007; revised manuscript received 25 September 2007; published 13 March 2008)

We study the magnetic properties of a system of interacting nanoparticles in a triangular lattice through Monte Carlo simulations. The small particles are subjected to an in-plane magnetic field and are coupled via long-range dipolar interactions. They also present uniaxial anisotropy energy, with the easy axes pointing randomly in three dimensions. We assume a Gaussian distribution for the strengths of the uniaxial anisotropy energy. We calculate the blocking temperature of the system from the zero-field-cooled curve as a function of the ratio between the dipolar and mean uniaxial anisotropy energy contributions. The blocking temperature increases linearly with this ratio, showing that the net effect of the dipolar interactions is to increase the height of the effective energy barriers seen by the nanoparticles. The hysteresis curves are also determined as a function of this ratio and we show that the coercive field exhibits a slight minimum for a small value of the dipolar strength. When the dipolar interactions are not negligible, we observe a steep variation in the component of the magnetization that is perpendicular to the magnetic field in the neighborhood of the coercive field.

DOI: [10.1103/PhysRevB.77.104419](https://doi.org/10.1103/PhysRevB.77.104419)

PACS number(s): 05.10.Ln, 75.50.Tt, 75.60.Jk, 75.20.-g

I. INTRODUCTION

Research on nanomagnetic systems is a topic of growing interest. The synthesis of new magnetic nanoparticles and their potential use in data recording and biosciences have been recently reviewed.^{1,2} Stoner and Wohlfarth,³ Néel,⁴ and Brown⁵ developed the initial studies on the magnetization reversal of single-domain particles with very large magnetic moments through thermal fluctuations across energy barriers. Their predictions could be confirmed after the production of nanostructured single-domain magnetic particles.⁶⁻⁸ Indeed, samples of high quality have been devised for which the individual nanoparticles are coated by nonmagnetic layers to prevent exchange coupling between nearest-neighbor particles.⁸⁻¹³ Each individual nanoparticle is formed by hundreds or thousands of atomic magnetic moments strongly coupled by exchange interactions. If the degree of dilution of the sample is very high, the nanoparticles do not interact, and their dynamics is dictated only by the external applied magnetic fields, effective uniaxial anisotropy, which include shape and magnetocrystalline contributions, and coupling with the heat bath.

On the other hand, this scenario changes completely when the dilution is not so low, and we need to include long-range magnetic dipolar forces between the nanoparticles to correctly describe the thermodynamical behavior of the system. Due to the presence of dipolar interactions, the otherwise purely uniaxial anisotropy energy barrier seen by each nanoparticle is modified. It is still a matter of debate in the literature how this change occurs. Even in the limit of weak dipolar interactions, in some experiments the blocking temperature increases¹⁴ with concentration, while in others it decreases.¹⁵

One question that is relevant in the discussion of the low-temperature properties of an array of magnetic dipoles is its underlying Bravais lattice structure. Luttinger and Tisza¹⁶ showed that the lowest energy state of a collection of classical dipoles is ferromagnetic in a face centered cubic lattice,

whereas it is antiferromagnetic in a simple cubic lattice. In two dimensions, it is well established that a square lattice of classical point dipoles exhibits an antiferromagnetic arrangement of the moments,^{17,18} while in the case of a triangular lattice, the arrangement is ferromagnetic.^{19,20}

Another question for which the answers appear to be conflicting is related to the role played by the dipolar interactions on the effective energy barrier seen by the nanoparticles. For instance, in the case of zero-field-cooled (ZFC) curves, the blocking temperature increases with the strength of the dipolar interactions, suggesting that the effective energy barrier seen by the nanoparticles also increases.²¹ On the other hand, in the case of the magnetic relaxation process from a saturated state, Iglesias and Labarta²² showed that for a linear chain of magnetic moments, the dipolar interactions effectively reduce the barrier height seen by the nanoparticles. Recently, we have considered a triangular array of identical magnetic nanoparticles with random uniaxial anisotropy axes in three dimensions and coupled by dipolar forces.²³ For this system, we have observed that, indeed, the effective energy barrier increases with the strength of the dipolar interactions in the case of ZFC curves, whereas it decreases in the relaxation processes. The effective energy barriers corresponding to the blocking temperature and to magnetization relaxation are different because the processes are different. While the initial state of the system is completely disordered in the ZFC experiments, it is fully ordered in the magnetic relaxation experiments.

The aim of this work is to determine the blocking temperature and the hysteresis curves for a system of magnetic nanoparticles in a two-dimensional triangular lattice through Monte Carlo simulations. We assume that the easy axes are randomly oriented in the three-dimensional space, the strength of the uniaxial anisotropy energies follows a Gaussian distribution, and the particles interact through a long-range magnetic dipolar interaction. The remanence and the coercive field are determined as a function of the ratio between the dipolar strength and the mean uniaxial anisotropy energy. Particularly interesting is the behavior of the coer-

cive field, which displays a slight minimum at low temperatures and for a small value of this ratio. We show that near the coercive field, the variation of the component of the magnetization that is transverse to the magnetic field is large and steep.

In our previous work,²³ we have applied our results to describe the magnetic properties of the magnetoferritin nanoparticles. There, we have estimated the ratio between the blocking temperatures of the most aggregated and well-dispersed magnetoferritin samples by assuming that all particles present identical energy barrier heights. Although we have found good agreement with the experimental results, our calculations were based on an effective energy barrier instead of using the experimental Gaussian distribution for the magnitude of the uniaxial anisotropies. In this paper, we get better results for the magnetoferritin system by taking into account its real distribution of energy barrier heights.

In the next section, we present the model and some details concerning the Monte Carlo simulations. In Sec. III, we present our results for the magnetic properties as a function of temperature and dipolar strength. In Sec. IV, we summarize our conclusions.

II. MODEL AND CALCULATIONS

Our particles are placed at the sites of a triangular lattice, which is assumed to lie in the xy plane. Each particle possesses a uniaxial anisotropy with its easy axis pointing randomly in the three-dimensional space. The magnitude of the anisotropy is given by $d=KV$, where K is the anisotropy energy per unit volume and V is the volume of the particle. We assume a Gaussian distribution for the magnitude of the anisotropies with mean value d_0 and standard deviation σ . For most of our calculations, we used $d_0=0.5$ and $\sigma=0.1$. As we will see below, this choice was made to yield good agreement with the experimental result for the ratio between the blocking temperatures of the most aggregated and well-dispersed samples of the magnetoferritin nanoparticles. If we keep the dipolar strength fixed, which is defined by the ratio between the magnetic dipolar coupling and uniaxial anisotropy, increasing d is equivalent to decreasing the ratio between the blocking temperatures of the most aggregated and well-dispersed samples. This fact can be appreciated in Fig. 6 of our earlier work.²³ The magnetic moment of the i th particle is written as $\boldsymbol{\mu}_i=\mu\mathbf{S}_i$, where \mathbf{S}_i is a unit vector, $|\mathbf{S}_i|=1$, and $\mathbf{S}_i=(S_{ix}, S_{iy}, S_{iz})$. We also write μ in the form $\mu=M_s V$, where M_s is the particle magnetization. An in-plane external magnetic field of magnitude H is applied along the x direction of the triangular lattice, which we choose to be parallel to a side of the conventional unit cell. The particles interact via a two-pair dipolar term, and the magnitude of the dipolar energy is written as a function of the parameter $g=\mu_0\mu^2/4\pi a^3$, where a is the lattice parameter. The corresponding Hamiltonian for a set of N particles is

$$\mathcal{H} = \frac{1}{2}g \sum_{i=1}^N \sum_{j \neq i}^N \left[\frac{\mathbf{S}_i \cdot \mathbf{S}_j}{r_{ij}^3} - 3 \frac{(\mathbf{S}_i \cdot \mathbf{r}_{ij})(\mathbf{S}_j \cdot \mathbf{r}_{ij})}{r_{ij}^5} \right] - \sum_{i=1}^N h S_{ix} - \sum_{i=1}^N d_i (\hat{e}_i \cdot \mathbf{S}_i)^2, \quad (1)$$

where r_{ij} is the distance separating the magnetic moments at

sites i and j , which is measured in units of the lattice parameter a , and $h=\mu H$. The vector \hat{e}_i is a vector of unit magnitude in the direction of the easy axis for the particle at site i . An important parameter to describe the effect of dipolar interactions on the magnetic properties of the system is the ratio $\alpha=g/d_0$.

This model is suitable to describe the magnetic properties of the magnetoferritin nanoparticles, which present a very narrow size distribution and the easy axes are randomly distributed over the sample. It is an interesting nanoparticle to probe the effect of the dipolar interactions because its 2 nm protein shell prevents contact between the magnetic cores of nearest-neighbor nanoparticles. Arrays of magnetoferritin particles were prepared on coated Cu transmission electron microscope (TEM) grids and studied by TEM and superconducting quantum interference device magnetometry.^{11,24} In the dispersed sample, the calculated mean interparticle separation was 130 nm, while in the aggregated sample, the magnetoferritin particles were in contact. The magnetoferritin particles are spherical with an average diameter of 12 nm, while the diameter of the magnetic core is $D=8$ nm. The estimated anisotropy energy is $d=5 \times 10^{-21}$ J, while its dipole moment is $\mu=1 \times 10^4 \mu_B$. Therefore, in the concentrated case, where particles touch each other, $a=12$ nm and the estimated value of α is 0.1. For the magnetoferritin system, the blocking temperatures of the well-dispersed and most aggregated samples are 22 and 28 K, respectively.

Studies on the magnetic properties of nanoparticles have been performed at zero temperature, exploring the hysteresis phenomenon and structure of the monolayer,^{19,25-27} and at finite temperatures, where besides hysteresis, other properties have also been investigated. Most of the calculations at finite temperature were performed by employing Monte Carlo simulations. For instance, the effects of packing geometries,²⁸ tunneling magnetoresistance,²⁹ reversible transverse susceptibility,³⁰ magnetic relaxation,^{22,31} and finite size effects^{32,33} are some of the problems that received attention in recent years.

We have employed Monte Carlo simulations to study the magnetic properties of the system. We have taken a system of linear size $L=21$ on a triangular lattice, with 441 magnetic moments, and we assumed free boundary conditions in our calculations. The role of the boundary conditions was considered in the works of Kechrakos and Trohidou^{28,29} as well as in our recent study of a system of identical magnetic nanoparticles.²³

The procedure we used to determine the equilibrium states of the system is based on the minimization of its free energy through the Monte Carlo technique and the well known Metropolis algorithm.³⁴ According to this algorithm, a given magnetic moment is selected at random, and we try to move it to a new position in such a way that the deviation from the old state is random, but within a maximum solid angle. We calculate the change in energy of the system (ΔE), and if $\Delta E \leq 0$, the transition to a different configuration is accepted. On the other hand, if $\Delta E > 0$, the transition to a different configuration is made with probability $\exp(-\Delta E/k_B T)$. This is the most expensive part of the simulation because, after the transition, we need to recalculate the dipolar field acting on all the other particles of the system. In

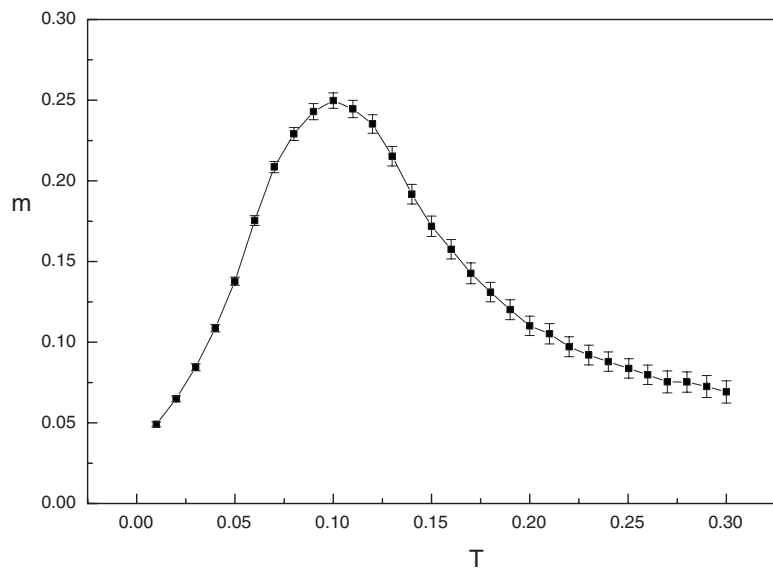


FIG. 1. Zero-field-cooled magnetization versus temperature for an interacting system ($\alpha=0.1$), and uniaxial anisotropy energy parameters $d_0=0.5$ and $\sigma=0.1$. The external magnetic field is $h=0.05d_0$. The error bars represent averages over 200 samples. The line serves as a guide for the eye.

each Monte Carlo step (MCs), we performed $N=441$ (N is the number of magnetic moments of the system) trials to flip the magnetic moments. To calculate the average magnetic properties, we considered 10^4 MCs, where the first 2×10^3 MCs were discarded due to the thermalization process. This number of MCs to reach the equilibrium state was achieved by taking a maximum solid angle variation equal to 0.1π , where approximately 50% of the attempted moves were successful. Due to the thermal fluctuations and the random direction of the easy axes, we have taken a minimum of 50 and a maximum of 200 samples to determine the thermal properties. On the other hand, each sample is selected for a ZFC experiment only when its initial total magnetization is less than 10^{-3} .

In our algorithm, we calculated the average magnetization per particle, as well as its components in the x , y , and z directions, as a function of temperature and ratio α . These average values were obtained, first, by calculating the mean values of the magnetic moments of the system for each MCs after the thermalization process as follows:

$$M_x = \frac{1}{N} \sum_{i=1}^N S_{ix}, \quad (2)$$

$$M_y = \frac{1}{N} \sum_{i=1}^N S_{iy}, \quad (3)$$

$$M_z = \frac{1}{N} \sum_{i=1}^N S_{iz}, \quad (4)$$

$$M_{\text{tot}} = \sqrt{M_x^2 + M_y^2 + M_z^2}. \quad (5)$$

Afterward, these averages were taken by considering all the Monte Carlo steps, after thermalization. Finally, an average is performed over all the selected samples.

III. RESULTS

We have determined the blocking temperature as a function of the parameter α by considering the corresponding zero-field-cooled curves for each value of this parameter. We apply a very small magnetic field in the x direction for each zero-field-cooled sample, where the initial magnetization is close to zero at very low temperatures. This field is chosen to be equal to 5% of d_0 , which is the mean barrier height due to the uniaxial anisotropy energy. Then, by increasing the temperature, some magnetic moments become unblocked and a net magnetization appears in the field direction. With a further increase in the temperature, the magnetization reaches a maximum value, which is defined as the blocking temperature of the system. For temperatures higher than the blocking temperature, the magnetization decreases for increasing values of the temperature and the system is in the superparamagnetic state.

We show in Fig. 1 the magnetization as a function of temperature for a Gaussian distribution of uniaxial anisotropy energies with $d_0=0.5$, $\sigma=0.1$, and dipolar interaction strength $\alpha=0.1$. We find a well defined peak in the magnetization curve at $T=0.10$. The temperature here is measured in units of d_0 , that is, T means $k_B T / d_0$, where k_B is the Boltzmann constant. The blocking temperature for the noninteracting system, $\alpha=0$, for the same values of the parameters d_0 and σ is equal to $T_0=0.08$. We have included in Fig. 1 the standard error for each value of the temperature. Assuming that the sample magnetization is Gaussian distributed, our estimate for the standard error is given by the expression

$$\epsilon = \sqrt{\frac{\sum_{i=1}^{n_s} (\delta m_i)^2}{n_s(n_s - 1)}}, \quad (6)$$

with $\delta m_i = m_i - m$, where m is the mean value of the magnetization for a set of n_s independent sample realizations, which account for the random direction of the easy axes and anisotropy energy distribution. The value of m_i for each sample is already the mean value taken over the Monte Carlo

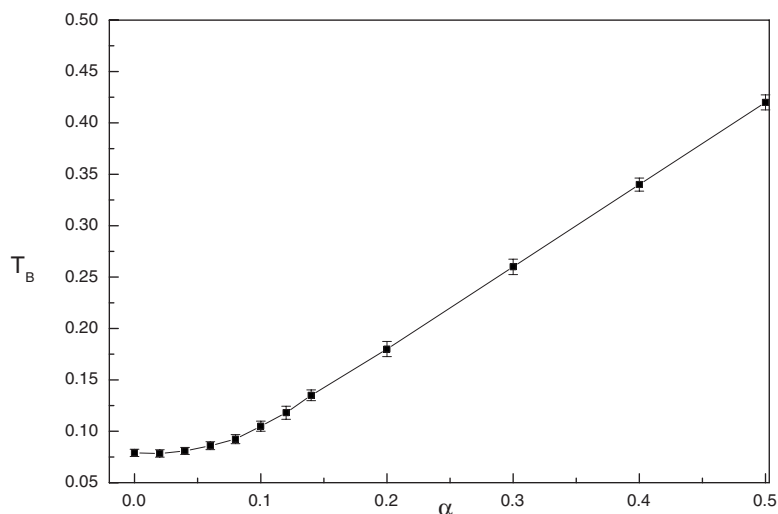


FIG. 2. Blocking temperature (T_B) as a function of the dipolar strength α . The error bars take into account 200 independent samples. The uniaxial anisotropy energy parameters are $d_0 = 0.5$ and $\sigma = 0.1$. The line serves as a guide for the eye.

steps of the simulation due to the thermal fluctuations. In Fig. 1, we have used $n_s = 200$. For temperatures well below the blocking temperature, the error bars are of the size of the symbols or smaller. However, due to the thermal fluctuations, the error bars are larger around the blocking and higher temperatures. Although not presented here, the susceptibility, specific heat, and Binder cumulant also show a maximum around the blocking temperature for $\alpha = 0$.²³

Figure 2 displays the plot of the blocking temperature as a function of the dipolar strength. For the range of values of α shown in Fig. 2, we see that the increase in the blocking temperature is smoother in the interval $0 < \alpha < 0.1$. However, for values of $\alpha > 0.1$, it increases linearly with the dipolar strength. The enhancement of the magnetic properties due to the dipolar interactions was observed in other studies. For instance, Lee *et al.*³⁵ found that the remanent magnetization is consistently higher for simulations with magnetostatic interactions as compared to simulations without magnetostatic interactions, even for a very diluted system of interacting point dipoles and uniaxial anisotropy with random axis in a plane.

As we have commented earlier, this model describes the magnetoferritin system very well.²⁴ The blocking temperatures of the well-dispersed and most aggregated samples are estimated to be 22 and 28 K, respectively. The mean distance between two nearest-neighbor particles in the well-dispersed sample is 130 nm, which gives $\alpha = 10^{-4}$, that is, the well-dispersed sample is noninteracting and we assume for it the value $\alpha = 0$. The estimated value for the most aggregated samples, where particles are in contact, is $\alpha = 0.1$. Figure 2 shows that, for $\alpha = 0.1$, the blocking temperature is $T = 0.10$, which gives the ratio of 1.25 between the blocking temperatures of the aggregated and well-dispersed samples, the value of which is very close to the experimental ratio (1.27). The increase in the magnitude of the dipolar interactions has the net effect of enhancing the effective energy barrier height seen by the nanoparticles in the ZFC experiments performed on samples with a triangular lattice arrangement of magnetic dipoles.

We have also observed that the plot of the ratio between the dipolar and uniaxial anisotropy energies versus tempera-

ture for $\alpha = 0.1$ is very similar to that seen in Fig. 1 for the magnetization. They present a maximum at the same temperature, which is the blocking temperature of the system. While the uniaxial anisotropy energy is an increasing function of temperature during the ZFC experiment, the dipolar energy decreases up to near the blocking temperature, where it exhibits a minimum.

Figure 3 shows two hysteresis curves for the noninteracting ($\alpha = 0$) and interacting ($\alpha = 0.3$) systems at a very low temperature ($T = 10^{-4}$). We observe that the remanence is approximately the same for both systems, while the coercive field is clearly larger for the interacting system. In order to better understand this behavior, we have calculated the remanence and coercivity as a function of α at very low temperatures. The remanence was determined by letting the magnetic moments of the system relax, in a zero external field, from an initial state where all the moments are aligned in the x direction, that is, the initial state is given by ($S_{ix} = 1$, $S_{iy} = 0$, $S_{iz} = 0$). We considered 10^4 MCs for the system to reach equilibrium, although at very low temperatures, equilibrium is easily achieved within 500 MCs. This happens because the initial state is one of high energy and the system simply relaxes toward equilibrium at very low temperatures, where thermal fluctuations are negligible. In this case, the acceptance rate is almost equal to 1.

Although the Monte Carlo simulation based on Metropolis algorithm is not the best method for the minimization of the total energy at very low temperatures, it has been used with success in the study of magnetic nanoparticles.²⁸⁻³⁰ When the initial state of the system is well ordered, with high energy, as happens in our case, the evolution to the lowest energy state is guaranteed because in each Monte Carlo step we explore only a small region of the phase space around the current state. If large random moment deviations were considered between successive Monte Carlo steps, we would have the formation of metastable clusters and the time to reach the minimum energy state would be very large. For instance, at the end of the relaxation, the magnetization of the noninteracting system is 1/2, which is the expected value for a random distribution of uniaxial axes in three dimensions. On the other hand, the mean deviation of the moments

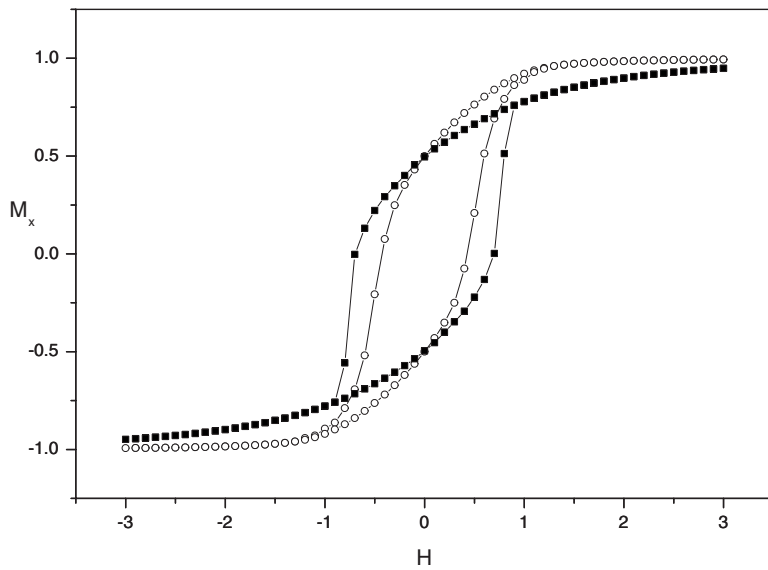


FIG. 3. Hysteresis loops for interacting ($\alpha = 0.3$, closed squares) and noninteracting ($\alpha = 0$, open circles) systems. The uniaxial anisotropy energy parameters are $d_0 = 0.5$, $\sigma = 0.1$, and $T = 10^{-4}$. The lines serve as a guide for the eye.

from their easy axis direction increases with the dipolar strength. While the mean deviation is zero for $\alpha = 0$, its value is 6° for $\alpha = 0.1$. At finite temperatures, we need at least 10^4 MCs to achieve equilibrium as we have seen during the ZFC experiments. We have also taken 200 samples to allow different realizations of the random axis and anisotropy energy distributions.

We show in Fig. 4 the remanence, which is defined by the component M_x of the total magnetization, as a function of α . We have also plotted in Fig. 4 the two other components of the total magnetization. The x component M_x slightly increases from the value $1/2$, which is the well known value for a noninteracting system with completely random uniaxial axes in three dimensions, up to near $\alpha = 0.1$, and then decreases again for $\alpha > 0.2$ to a value close to $1/2$. As expected, the out of plane component M_z is almost zero even for the noninteracting case. However, while the x and z components of total magnetization are nearly independent of the dipolar strength, the transverse component of the magnetization M_y is an increasing function of α and assumes large values even

for small values of the dipolar strength. In order to appreciate the effect of temperature in relaxation, we plot in Fig. 5 the x component of total magnetization as a function of the dipolar strength for the temperatures $T = 10^{-4}$ and $T = 0.05$. For small values of the dipolar strength, the values of the remanence are quite different. However, they approach each other as we increase the dipolar strength, despite the rather distinct values of the considered temperatures.

The coercivity is defined by the value of the external magnetic field for which the x component of the magnetization, at the end of the simulation, changes its sign after we start from the uniform distribution of magnetic dipoles ($S_{ix} = 1, S_{iy} = 0, S_{iz} = 0$) at $t = 0$. The external magnetic field is applied in the negative x direction. We also considered 200 different samples and waited 10^4 MCs to determine the coercive field. In Fig. 6, we plot the coercive field as a function of α and we observe the presence of a slight minimum around $\alpha = 0.1$. The decrease is only 2% relative to the noninteracting case. We had observed a larger decrease (13%) in the case of a system of identical nanoparticles.²³ Figure 7 is

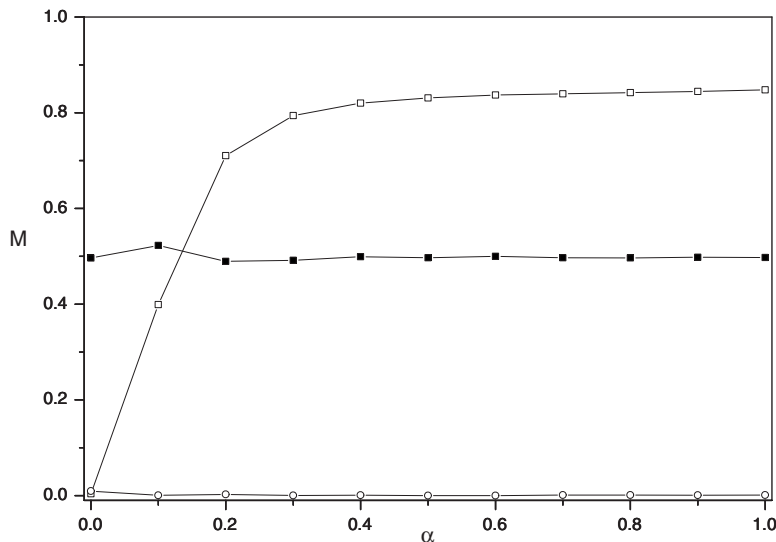


FIG. 4. Absolute value of the components of total magnetization as a function of the dipolar strength: M_x (closed squares), M_y (open squares), and M_z (open circles). The uniaxial anisotropy energy parameters are $d_0 = 0.5$, $\sigma = 0.1$, and $T = 10^{-4}$. The lines serve as a guide for the eye.

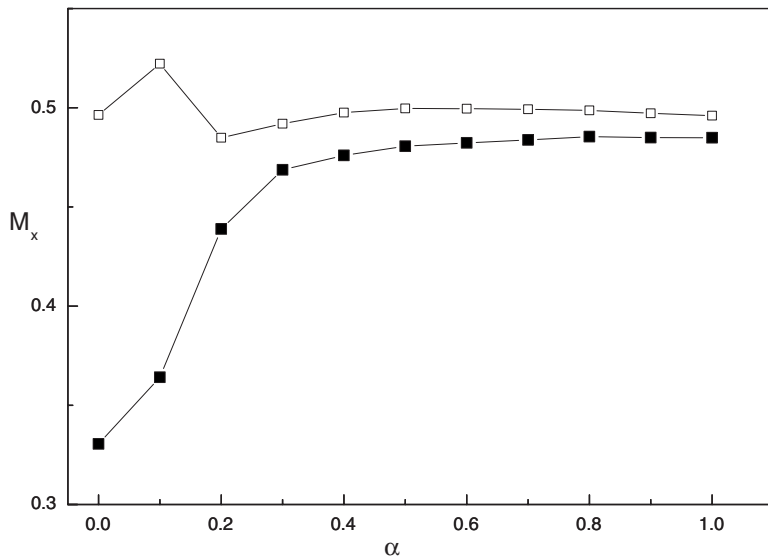


FIG. 5. Absolute value of the x component of total magnetization as a function of the dipolar strength for temperatures $T=10^{-4}$ (open squares) and $T=0.05$ (closed squares). The uniaxial anisotropy energy parameters are $d_0=0.5$ and $\sigma=0.1$. The lines serve as a guide for the eye.

a detailed view of the coercive field for small values of the dipolar strength. The error bars in the figure are determined from a set of 200 independent samples. Indeed, within the statistical errors, the minimum is observed for the value $\alpha=0.10$. In order to give support to the use of the Metropolis Monte Carlo algorithm at low temperatures, we also considered a purely dipolar case with $d_0=0$ and $g=1$. For this system in the triangular lattice, we find for the coercive field the value $H_c=1.98$, which is very close to $H_c=1.87$ found by Russier¹⁹ through the minimization of the dipolar energy at zero temperature.

We show in Fig. 8 the plot of the component of total magnetization transverse to the field when $M_x=0$. Even for small values of α , it assumes a large value. For instance, its value rises from zero for $\alpha=0$ to a value close to 0.30 for $\alpha=0.10$, where the coercive field attains its minimum value. Besides, this transverse component saturates for dipolar strength values larger than 0.30. We believe that the unusual behavior we find for the coercive field at very low tempera-

tures is due to the use of free boundary conditions in our simulations, where demagnetization effects were not taken into account. For instance, in a triangular lattice, calculations assuming periodic boundary conditions¹⁹ predict a decreasing coercive field as a function of the dipolar strength, although the decrease is not as strong for large values of the dipolar strength.

It is interesting to note that other properties also present a peculiar behavior near the coercive field at very low temperatures. We show in Fig. 9 the behavior of dipolar and uniaxial anisotropy energies as a function of α at the coercive field for which $M_x=0$. Like the coercive field, the uniaxial anisotropy energy also displays a very slight minimum at the value $\alpha=0.1$. On the other hand, the dipolar energy is a monotonically decreasing function of α . Then, the triangular array of magnetic moments behaves as a true ferromagnetic state even for small values of the dipolar strength.

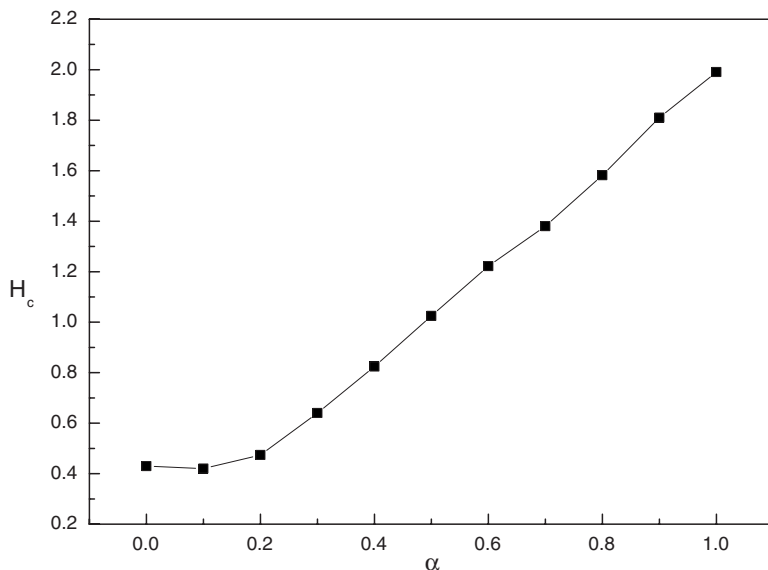


FIG. 6. Coercive field as a function of the dipolar strength. The uniaxial anisotropy energy parameters are $d_0=0.5$, $\sigma=0.1$, and $T=10^{-4}$. The line serves as a guide for the eye.

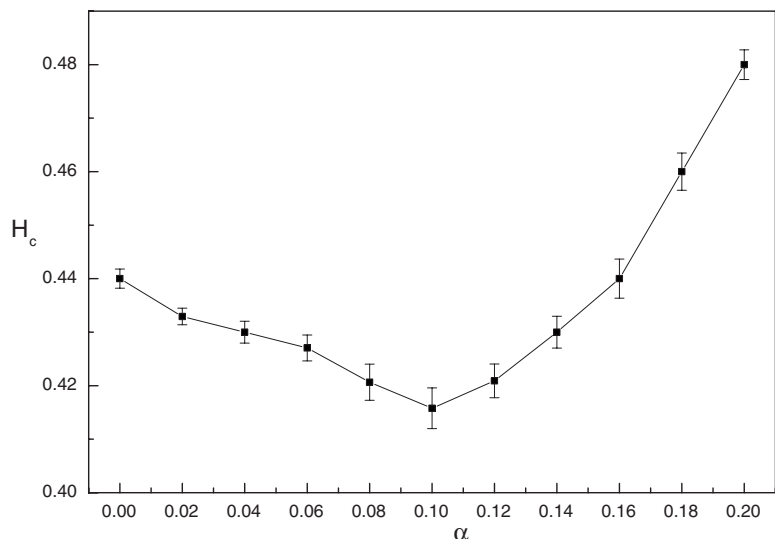


FIG. 7. Detailed view of Fig. 6 for small values of the dipolar strength showing the minimum at $\alpha=0.10$. The error bars are calculated from a set of 200 independent samples. The line serves as a guide for the eye.

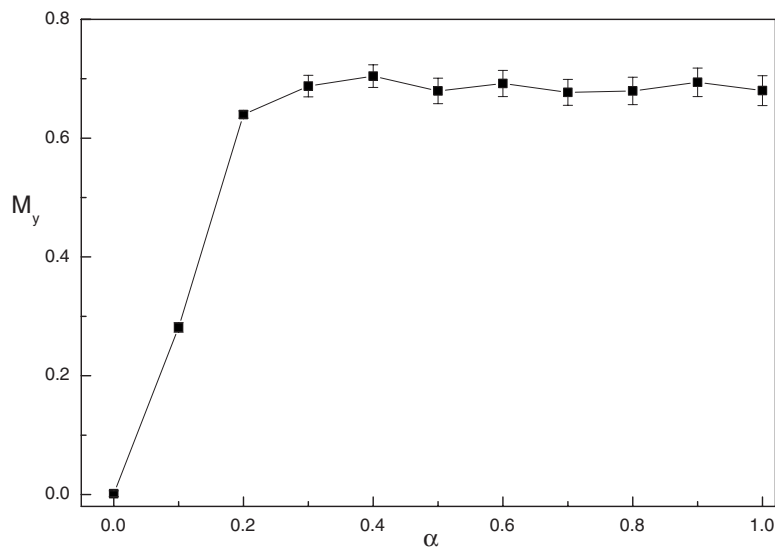


FIG. 8. The M_y component of total magnetization at the coercive field for which $M_x=0$. The uniaxial anisotropy energy parameters are $d_0=0.5$, $\sigma=0.1$, and $T=10^{-4}$. The error bars are calculated from a set of 200 independent samples.

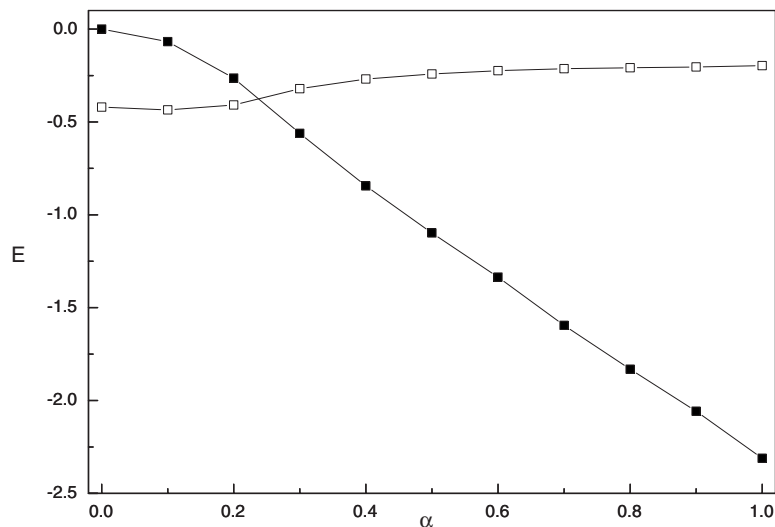


FIG. 9. Uniaxial anisotropy (open squares) and dipolar (closed squares) energies per particle, calculated at the coercive field, as a function of the dipolar strength. The uniaxial anisotropy energy parameters are $d_0=0.5$, $\sigma=0.1$, and $T=10^{-4}$. The lines serve as a guide for the eye.

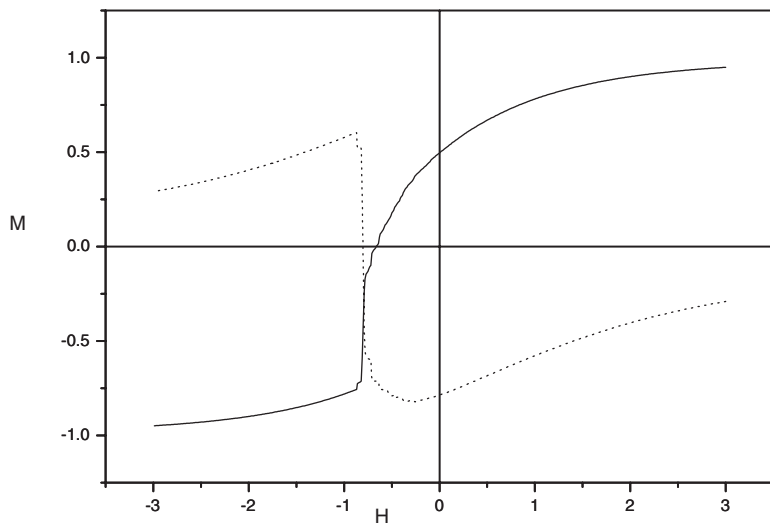


FIG. 10. M_x (solid line) and M_y (dotted line) components of total magnetization for $\alpha=0.3$. The uniaxial anisotropy energy parameters are $d_0=0.5$, $\sigma=0.1$, and $T=10^{-4}$.

We show in Fig. 10 the longitudinal M_x and transverse M_y components of total magnetization as a function of the magnetic field for the particular value $\alpha=0.3$. Figure 10 corresponds to one-half of the hysteresis loop at temperature $T=10^{-4}$, and we have removed the points for clarity. By increasing the field from negative values, we found that the transverse component of the magnetization jumps abruptly just before we reach the coercive field. A similar behavior is also seen for other values of the dipolar strength.

Finally, we show in Fig. 11 the behavior of the coercive field as a function of temperature for selected values of the dipolar strength. The coercive field decreases with temperature for any value of α . At the smallest temperatures, the behavior is similar to that presented in Fig. 6, where the coercive field attains its minimum value for $\alpha=0.1$. Due to this fact, as we increase the temperature, the curves for $\alpha=0$ and $\alpha=0.1$ cross because the decay is slower for the interacting systems. The blocking temperature can also be estimated from these plots. It is the temperature above which the coercive field vanishes. The value of the blocking temperature determined using this procedure is slightly larger

than the one found from the peak of the magnetization in the ZFC experiments, which is given in Fig. 2.

IV. CONCLUSIONS

We have studied in this work the magnetic properties of a system of interacting magnetic nanoparticles in a triangular lattice. The particles interact via long-range dipolar forces and their uniaxial anisotropy axes are uniformly distributed in three dimensions. We have also assumed that the anisotropy energy strength is distributed according to a Gaussian probability function. We have employed in our calculations the Monte Carlo method along with the Metropolis prescription to sweep over the phase space of the system, and we assumed free boundary conditions. From the measurements of the magnetization as a function of temperature in the ZFC experiments, we determined the blocking temperature as a function of the ratio between the dipolar strength and the mean uniaxial anisotropy energy. We have shown that the blocking temperature increases linearly with this ratio. The increase in the blocking temperature with dipolar strength

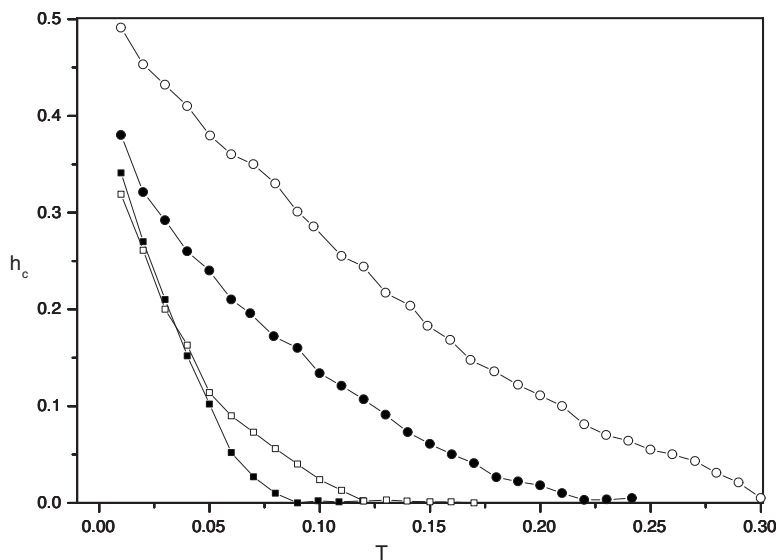


FIG. 11. Coercive field as a function of temperature: $\alpha=0$ (solid squares), $\alpha=0.1$ (open squares), $\alpha=0.2$ (solid circles), and $\alpha=0.3$ (open circles). The uniaxial anisotropy energy parameters are $d_0=0.5$ and $\sigma=0.1$. The lines serve as a guide for the eye.

indicates that the dipolar interactions effectively enhance the height of the energy barriers seen by the nanoparticles. We have also determined the hysteresis curves as a function of the dipolar strength. The coercive field is a decreasing function of temperature for any value of the dipolar strength. However, at very low temperatures, it exhibits a slight minimum as a function of the dipolar strength. In the case of interacting systems, close to the coercive field, we observe a steep variation in the component of total magnetization that

is transverse to the magnetic field. We have seen that this model appears to be adequate in describing the magnetic properties of the magnetoferritin nanoparticles.

ACKNOWLEDGMENTS

W.F. acknowledges support from the Brazilian agency CNPq.

-
- ¹L. Machala, R. Zboril, and A. Gedanken, *J. Phys. Chem. B* **111**, 4003 (2007).
²P. Tartaj, *Curr. Nanosci.* **2**, 43 (2006).
³E. C. Stoner and E. P. Wohlfarth *Philos. Trans. R. Soc. London, Ser. A* **240**, 599 (1948).
⁴L. Néel, *Ann. Geophys. (C.N.R.S.)* **5**, 99 (1949).
⁵W. F. Brown, *J. Appl. Phys.* **30**, 130S (1959).
⁶*Science and Technology of Nanostructured Magnetic Materials*, edited by G. C. Hadjipanayis and G. A. Prinz (Plenum, New York, 1991).
⁷M. A. Willard, L. K. Kurihara, E. E. Carpenter, S. Calvin, and V. G. Harris, *Int. Mater. Rev.* **49**, 125 (2004).
⁸J. L. Dormann, D. Fiorani, and E. Tronc, *Adv. Chem. Phys.* **98**, 283 (1997).
⁹C. Petit, A. Taleb, and M. P. Pileni, *J. Phys. Chem.* **103**, 1805 (1999).
¹⁰X. M. Lin, C. M. Sorensen, K. J. Klabunde, and G. C. Hadjipanayis, *Langmuir* **14**, 7140 (1998).
¹¹F. C. Meldrum, B. R. Heywood, and S. Mann, *Science* **257**, 522 (1992).
¹²K. K. W. Wong, T. Douglas, S. Gider, D. D. Awschalom, and S. Mann, *Chem. Mater.* **10**, 279 (1998).
¹³J. M. Vargas, W. C. Nunes, L. M. Socolovsky, M. Knobel, and D. Zanchet, *Phys. Rev. B* **72**, 184428 (2005).
¹⁴W. Luo, S. R. Nagel, T. F. Rosenbaum, and R. E. Rosensweig, *Phys. Rev. Lett.* **67**, 2721 (1991).
¹⁵S. Morup and E. Tronc, *Phys. Rev. Lett.* **72**, 3278 (1994).
¹⁶J. M. Luttinger and L. Tisza, *Phys. Rev.* **70**, 954 (1946).
¹⁷A. B. MacIsaac, J. P. Whitehead, K. De'Bell, and P. H. Poole, *Phys. Rev. Lett.* **77**, 739 (1996).
¹⁸K. De'Bell, A. B. MacIsaac, I. N. Booth, and J. P. Whitehead, *Phys. Rev. B* **55**, 15108 (1997).
¹⁹V. Russier, *J. Appl. Phys.* **89**, 1287 (2001).
²⁰P. Politi, M. G. Pini, and R. L. Stamps, *Phys. Rev. B* **73**, 020405(R) (2006).
²¹X. X. Zhang, G. H. Wen, G. Xiao, and S. Sun, *J. Magn. Magn. Mater.* **261**, 21 (2003).
²²O. Iglesias and A. Labarta, *Phys. Rev. B* **70**, 144401 (2004).
²³W. Figueiredo and W. Schwarzacher, *J. Phys.: Condens. Matter* **19**, 276203 (2007).
²⁴A. P. Robinson, Ph.D. thesis, University of Bristol, 2005.
²⁵D. A. Dimitrov and G. M. Wysin, *Phys. Rev. B* **50**, 3077 (1994).
²⁶D. A. Dimitrov and G. M. Wysin, *Phys. Rev. B* **51**, 11947 (1995).
²⁷V. Russier, C. Petit, and M. P. Pileni, *J. Appl. Phys.* **93**, 10001 (2003).
²⁸D. Kechrakos and K. N. Trohidou, *Phys. Rev. B* **58**, 12169 (1998).
²⁹D. Kechrakos and K. N. Trohidou, *Phys. Rev. B* **71**, 054416 (2005).
³⁰D. Kechrakos and K. N. Trohidou, *Phys. Rev. B* **74**, 144403 (2006).
³¹L. Balcells, O. Iglesias, and A. Labarta, *Phys. Rev. B* **55**, 8940 (1997).
³²V. S. Leite and W. Figueiredo, *Phys. Lett. A* **359**, 300 (2006).
³³V. S. Leite, B. C. S. Grandi, and W. Figueiredo, *Phys. Rev. B* **74**, 094408 (2006).
³⁴D. P. Landau and K. Binder, *A Guide to Monte Carlo Simulations in Statistical Physics* (Cambridge University Press, Cambridge, 2000).
³⁵H. K. Lee, T. C. Schulthess, D. P. Landau, G. Brown, J. P. Pierce, Z. Gai, G. A. Farnan, and J. Shen, *J. Appl. Phys.* **91**, 6926 (2002).